www.czasopisma.pan.pl PAN POLSKA AKADEMIA NAUK www.journals.pan.pl

A R C H I V E S O F M E T A L L U R G Y A N D M A T E R I A L S

Volume 60 2015 Issue 4

DOI: 10.1515/amm-2015-0456

A. LISIECKI*#

WELDING OF THERMOMECHANICALLY ROLLED STEEL BY YB:YAG DISK LASER

SPAWANIE STALI WALCOWANEJ TERMOMECHANICZNIE LASEREM DYSKOWYM YB:YAG

Autogenous laser welding of 5.0 mm thick butt joints of thermomechanically rolled steel S700MC was investigated. The Yb:YAG disk laser TruDisk 3302 emitted at 1.03 μm was used for the trials of autogenous welding. The effect of laser welding parameters and thus thermal conditions of welding on weld shape, microstructure of weld metal and heat affected zone (HAZ), tensile strength, bending angle, impact toughness and microhardness profile was determined. Studies have shown that it is advantageous to provide a high welding speed and low heat input. High cooling rate of weld metal and HAZ leads to the formation of a favorable structure characterized by a large proportion of fine-grained acicular ferrite and provides high mechanical properties of butt joints.

Keywords: thermomechanically rolled steel, welding, disk laser

W artykule opisano wyniki badań procesu spawania laserowego bez materiału dodatkowego złączy doczołowych o grubości 5.0 mm ze stali walcowanej termomechanicznie S700MC. Próby spawania wykonano za pomocą lasera dyskowego Yb:YAG TruDisk 3302, który emituje promieniowanie o długości fali 1.03 μm. Badano wpływ parametrów spawania laserowego, a głównie warunków cieplnych procesu spawania na kształt ściegu spoiny, mikrostrukturę metalu spoiny i strefy wpływu ciepła (SWC), wytrzymałość na rozciąganie, kąt gięcia, udarność oraz rozkład mikrotwardości. Wyniki badań wskazują, że korzystne jest zapewnienie dużej prędkości spawania przy jednocześnie niskiej energii liniowej spawania. Duże szybkości stygnięcia metalu spoiny i SWC prowadzą do utworzenia korzystnej drobnoziarnistej struktury o dużym udziale ferrytu drobno płytkowego, co zapewnia wysokie właściwości mechaniczne złączy doczołowych.

1. Introduction

Modern fine-grained, thermomechanically rolled steels characterized by high yield point are increasingly used in the industry because of the many advantages and the desire to reduce weight and increase structural strength and reliability [1-3]. However, the performance of the structure depends on the weakest link, which is usually a welded joint [4-6]. The structural fine-grained, thermomechanically rolled steels with yield point up to 700 MPa have extremely low content of alloying elements mainly Nb, Ti, V, Zr, B etc. [3,7-9]. The total amount of Nb, V and Ti is limited to 0.15%. The Ti content does not exceed 0.015% in order to prevent the grain growth and loss of strength and toughness in the heat affected zone of welded joint (HAZ). Due to the extremely low content of alloying elements, these steels are commonly called microalloyed steels [3,10]. Additionally, these steels are characterized by low carbon equivalent, e.g. CEV 0.38 and CET 0.25 in a case of the lowest thickness (e.g. DOMEX 700MC) [3,11]. The thermomechanically rolled steels, especially the grade 700MC, are often mistakenly compared to the quenched and tempered steels S690Q (e.g. WELDOX 700) although they have a different chemical composition and thus different carbon equivalent and additionally their mechanical properties are obtained in different ways [3,12,13]. The differences in the value of carbon equivalent of the mentioned above steel grades are given in the Table 1. However, it should be noted that in practice the differences in the carbon equivalent values can be considerably higher, as shown by Górka J. [14]. Mechanical properties of the thermomechanically rolled steels are shaped in the complex technology of Thermo-Mechanical Control Processing (TMCP), as shown in Fig. 1 [3]. This technology provides a two phase microstructure consisting of very fine ferrite grains and bainite and/or martensite, depending on the processing conditions [3,14-17].

* SILESIAN UNIVERSITY OF TECHNOLOGY, FACULTY OF MECHANICAL ENGINEERING, WELDING DEPARTMENT, 18A KONARSKIEGO STR., 44-100 GLIWICE, POLAND

Corresponding author: aleksander.lisiecki@polsl.pl

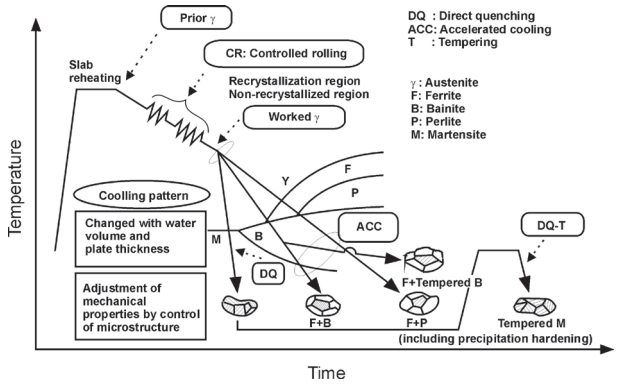

Fig. 1. Schematic illustration of thermomechanical rolling of microalloyed steels (TMCP) [3]

Due to the low carbon equivalent, the fine-grained, thermomechanically rolled steels are considered to be good weldable [1,2,14,18]. According to the steel manufacturer's instructions all conventional arc welding methods can be successfully used for welding of the modern thermomechanically rolled, microalloyed steels [3,14].

Moreover some of the steel manufactures recommend low-hydrogen welding methods. Additionally the only criterion for welding procedure (method of welding, parameters of welding, as well as the filler metal) is ensuring the tensile strength of joint not less than the tensile strength of the base metal (BM) [1,2]. However welding of these steel grades at too high heat input, especially during submerged arc welding, and also GMA welding may lead to significant decrease of plasticity and toughness of the welded joints, increase susceptibility to brittle fracture and fatigue as a result of harmful structural changes, creation of coarse structure of the weld metal and significant grain growth in the heat affected zone (HAZ) [14,19,20].

Many researchers have shown that in the case of welding of the fine-grained and especially ultra-fine grained steels by conventional arc welding methods such as GMA (gas metal arc welding) or SAW (submerged arc welding) the heat input has a significant influence on the mechanical performance of weld joint [21,22] The studies showed that the grain coarsening in heat affected zone (HAZ) may cause the performance mismatch between HAZ and base metal (BM) decreasing the mechanical performance of weld joint dramatically [14,21]. Therefore, new technologies of welding are being developed that provide high performance and relatively low heat input of welding. An example of a cutting-edge technology of microalloyed steel welding is the technology of GMA welding with micro-jet cooling elaborated by Węgrzyn T. and Piwnik J. [4,6,23,24]. They showed that the micro-jet cooling can significantly increase the cooling rate of weld metal and thus increase the percentage of acicular ferrite in the weld metal. Other promising technologies of welding the microalloyed, thermomechanically rolled steels are laser beam welding (LBM) and laser hybrid welding (LHW) [21,25,26]. These technologies are now widely investigated. Laser beam welding has many advantages such as low heat input, very narrow heat affected zone (HAZ), low thermal stresses and distortion, high quality of joints, high speed welding and deep penetration [25,27]. Until recently, for laser welding of steel joints just CO_2 (λ=10.6 μm) and diode-pumped Nd:YAG (λ=1.064 μm) lasers were used. On the other hand, the dynamic progress in design and development of laser devices have led to the introduction of new types of lasers for welding industry, such as a fiber and disk laser. These new types of lasers have many advantages compared to previously used industrial workhorse CO_2 and Nd:YAG lasers as showed by Sharma R. [28,29]. The mechanism of autogenous laser welding at keyhole mode is incomparable to the mechanisms of arc welding with an additional material [1,5,30]. The heat input of laser welding is many times lower and the cooling rates of weld metal and HAZ are very rapid [1,30]. Grajcar A. and Różański M. et al. investigated the keyhole welding of thermomechanically rolled steel sheets 2.0 mm thick by the Yb:YAG disk laser with output power of 12 kW [31]. They found that the thermal cycle of laser welding is extremely dynamic and it strongly influences the structural changes and microhardness of weld metal and HAZ.

Thus, it is clear that the development of laser welding technology of modern microalloyed steels with application of new types of lasers requires detailed investigations of the influence of the laser beam characteristic and processing parameters on the stability of the welding process and properties of welded joints [32,33].

Therefore, the study of laser welding of thermomechanically rolled steel sheet S700MC with a thickness of 5.0 mm was carried out by the modern disk laser TruDisk 3302 manufactured by TRUMPF.

The effect of laser welding parameters, especially heat input, on the microstructure of fusion zone and heat affected zone, hardness distribution, mechanical properties such as tensile strength, bending angle and also impact toughness of test joints have been evaluated.

2. Material and experimental procedure

The grade S700MC thermomechanically rolled steel was chosen for the study of autogenous laser welding of butt joints, Fig. 2. Samples in dimension of 100.0 x 100.0 mm were cut from 5.0 mm thick plate by means of industrial 2D cutting machine equipped with a CO_2 laser. The chemical composition and mechanical properties of the investigated steel are given in the Table 1 and 2. Surfaces of steel samples were sandblasted and next mechanically cleaned by a brush with stainless steel wires and finally cleaned by acetone just before the trials of laser welding. The surfaces were prepared in such a way that all the samples had same surface finish. The steel samples were mounted in a fixture as shown in Fig. 3. The weld configuration was set as square groove, butt joint (I-joint type) and tightly clamped to eliminate any distortion or displacement during laser welding, Fig. 3b. The area of laser beam interaction and the surface of a weld pool were protected by argon shielding delivered by a cylindrical nozzle set in front of the weld pool as shown in Fig. 3b. Argon flow was kept at 12.0÷15.0 l/min. Additionally the weld root was protected by argon delivered via a grove in a cooper backing of the fixture device. Argon flow from the root side was kept at approx. 3.0 l/min. The specific disk laser used for welding tests was Yb:YAG TruDisk 3302 manufactured by TRUMPF with maximum output power 3300 W and beam quality (beam parameter product - BPP) of

TABLE 1
Chemical composition of thermomechanically rolled steel S700MC according to EN 10149 –2 and comparison to DOMEX 700MC and WELDOX 700, Table 2, Fig. 2

Steel grade	Content % wt.														CET1)
	C	Mn	Si	Mo	V	Nb	Ti	Al	P	S	B	Cr	Cu	Ni	
S700MC Accord. to EN-10149-3	max 0.12	max 2.10	max 0.60	max 0.50	max* 0.20	max* 0.09	max* 0.22	max 0.015	max 0.025	max 0.015	max 0.005	-	-	-	0.38
DOMEX 700MC	max 0.12	max 2.10	max 0.10	-	max 0.20	max 0.09	max 0.15	min 0.015	max 0.025	max 0.010	-	-	-	-	0.33
WELDOX 700	max 0.20	max 1.60	max 0.60	max 0.70	-	-	-	-	max 0.020	max 0.010	max 0.005	max 0.70	max 0.30	max 2.0	0.53

Remarks; *Nb+Ti+V ≤ 0.22 %, 1) – comparison of the maximum values of carbon equivalent CET, DOMEX and WELDOX are SSAB's trade names

8.0 mm·mrad. The laser beam emitted at a wave length of 1.03 µm was delivered into the welding head via fiberglass with a core of 200 µm in diameter, Fig. 3a, Table 3. The fiberglass was coupled with the welding head by a collimator equipped with a 200 mm collimator lens. The laser beam was focused by a 200 mm focusing lens to a diameter of 200 µm. Technical data of the disk laser and focusing optics are given in Table 3.

The disk laser generator and beam transmission was controlled by a master control of a prototype, 4-axis fully automated positioning system based on three linear drives in the Cartesian coordinate system "x,y,z" and additionally with a rotary drive axis "a" as shown in Fig. 3a. The laser welding head was mounted vertically on a linear drive in the "z" direction (z axis). The linear drive "z" was used just to set the required distance from the laser head, which was perpendicular to the direction of welding and to the steel plate surface. During the trials of laser welding the laser head was stationary, while the plates to be welded were moved in a horizontal plane "x,y", driven be two linear stages ("x,y").

The welding parameters for autogenous laser welding were established in previous investigations on the influence of basic parameters of laser welding on the penetration characteristics and porosity formation in the weld metal during bead-on-plate laser welding. Results of these studies are described in detail in the ref 34. The laser beam was focused on the top surface of steel sheets (200 µm spot size) and the beam spot was relatively moved along the edges of the steel plates during welding. Welded joints have been created as a result of melting of the steel sheets edges and subsequent solidification of the liquid metal, without an additional material (filler). The test butt joints were one-side welded at parameters and technological conditions given in Table 4.

TABLE 2
Mechanical properties of thermomechanically rolled steel S700MC according to EN 10149 –2, Table 1

Nominal thickness, mm	**< 3**	**≥ 3**
Total elongation, A80 or A5, %	A80 10	A5 12
Minimum yield strength ReH, MPa	≥ 700	
Tensile strength Rm, MPa	750÷950	
Notch impact energy at -20°C, KV, J	≥ 40	
Notch impact energy at -40°C, KV, J	≥ 27	

TABLE 3
Technical data of the Yb:YAG TruDisk 3302 laser and the focusing optics, Fig. 3

Parameter	Value
Wave length, nm	1030
Maximum output power, W	3300
Laser beam divergence, mm·mrad	<8.0
Fiber core diameter, µm	200.0
Collimator focal length, mm	200.0
Focusing lens focal length, mm	200.0
Beam spot diameter, µm	200.0
Fiber length, m	20.0

When the laser welding tests were completed, first the visual inspection were performed according to PN-EN 970 standard and then samples for further metallographic examinations were cut perpendicularly to the joint axis at the mid-length of the joint away from the region of initiation and completion of welding process.

The samples were mounted in resin (chemically hardened), grinded and polished then etched by Nital solution (3.0%) to reveal the fusion zone shape, heat affected zone width and microstructure of the welded joint. The metallographic examinations were based on macrostructure and microstructure observations using a light microscope, scanning electron microscope (SEM) and chemical analysis by energy dispersive X-ray spectroscopy (EDS). Microhardness was measured on the polished samples across the weld using a Vicker's tester at a load 200 g according to PN-EN 1043-2:2000 standard. Further, tensile tests of the laser welded joints were performed according to the PN-EN 895 standard, at room temperature. The tensile test samples were cut perpendicularly to the joint axis and shaped by milling with intensive water cooling, to avoid the effect of heat on the performance of test samples. They were 35.0 mm wide at the grip region and 25.0 mm wide in the mid region. Two tensile samples were tested for each laser welded joint and the fracture surfaces were further examined by scanning electron microscope (SEM) to identify ductile or brittle fracture mode.

TABLE 4

Parameters of autogenous laser welding of 5.0 mm thick butt joints of S700MC steel by disk laser TruDisk 3302, Fig. 3, Table 1-3

Test butt joint	Output laser power (W)	Welding speed (mm/min) (mm/s)	Heat input (J/mm)	Width of the weld face (mm)	Width of the weld root (mm)	Remarks
A	3300	1500 (25)	132	1.98	1.35	PP,GL, UF
B	2500	500 (8.33)	300	3.6	2.3	PP,GL
C	3300	1000 (16.6)	198	2.9	1.8	PP,GL, UF

Remarks, other parameters of butt joints laser welding: wavelength of laser radiation 1.03 µm, focal length of focusing lens: 200.0 mm, focal length of collimator lens: 200.0 mm, fiber core diameter: 200.0 µm, nominal beam spot diameter: 200.0 µm, shielding nozzle diameter: 8.0 mm, shielding gas: Ar (99.999%), gas feed rate on the top surface (face of weld): 10.0-12.0 l/min, gas feed rate from root side: 3.0 l/min, Quality assessment of the welds: FP – full penetration, FF – flat wed face, UF – undercut of wed face

Technological bend tests of the laser welded joints were performed on samples having a width of 20.0 mm according to the PN-EN 910:1999. Samples for the bend test were cut in the same way as the samples for tensile tests, perpendicularly to the joint axis.

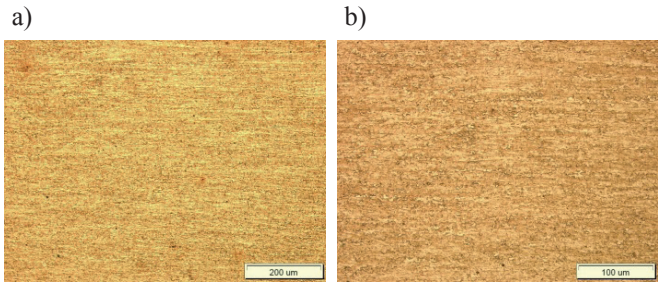

Fig. 2. Microstructure of the base metal (BM) of the 5.0 mm thick S700MC steel sheet at different magnification, 3% Nital etched, Table 1

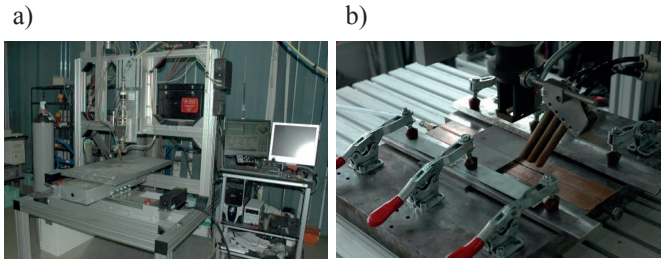

Fig. 3. A view of the prototype experimental stand for automated laser welding (a) equipped with the fixture device and shielding nozzles for protection of weld pool and root of the weld (b), Table 3

Finally, the impact test were performed according to PN – EN 10045-1 standard. Two impact test samples were prepared and tested for each laser welded joint. Result of the tests, measurements and analysis are given on the Fig. 4 to 11 and in the Table 4 to 8.

3. Results and discussion

All the test butt joints produced by autogenous laser welding using the disk laser are fully penetrated over the entire length, as shown in Fig. 4 and 5. The fusion zone shapes (configuration) as well as width of weld faces and roots of the butt joints are similar to the bead-on-plate welds produced at the same parameters and discussed in the ref 34, Table 4, Fig. 5. The butt joint B welded at laser power 2.5 kW and welding speed 500 mm/min, thus heat input 300 J/mm, showed smooth and even surfaces of the face and root as well, slightly convex but without undercuts, Fig. 4b and 5b. Fusion zone shape is proper, although single and small size pores with a diameter below 0.15 mm were found on the cross-sections, Fig. 5b. The butt joint C welded at laser power 3.3 kW and welding speed 1000 mm/min, thus heat input almost 200 J/mm, showed flat and even surface of the root but slight undercuts of the weld face, Fig. 5c. Fusion zone in X configuration also is proper but some small pores were found on the cross-sections with a maximum diameter below 0.1 mm, Fig. 5c. The butt joint A welded at minimum heat input of about 130 J/mm, at laser power 3.3 kW and welding speed 1500 mm/min, showed rather a columnar shape at the depth/width ratio about 2.5, Fig. 5a. Surface of the root is flat and even but the weld face is slightly hollowed, Fig. 4a.

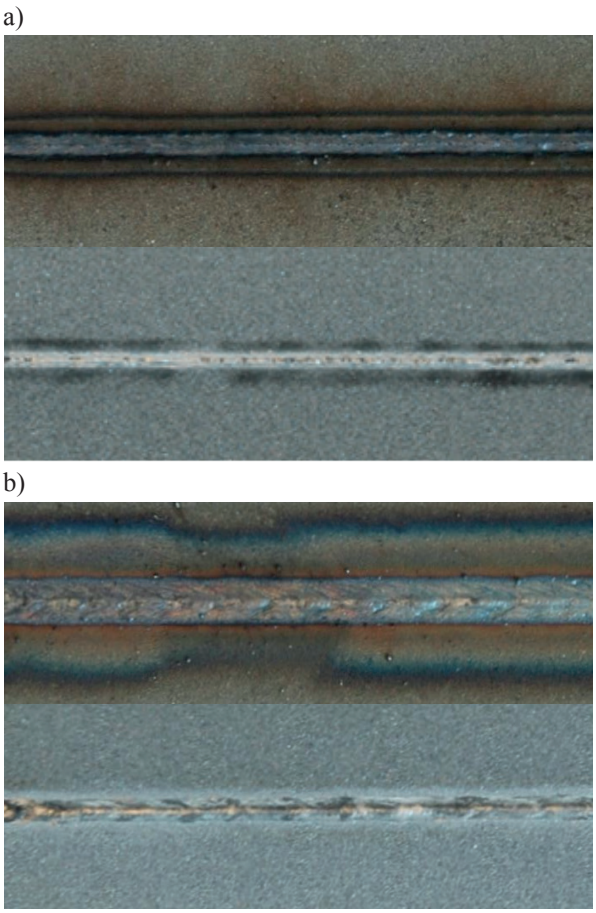

Fig. 4. A view of the weld face (top surfaces) and root (bottom) of the 5.0 mm thick butt joints of S700MC steel produced by autogenous laser welding (Table 4); a) at minimum heat input of 132 J/mm (3.3 kW, 1.5 m/min), joint A and b) at maximum heat input of 300 J/mm (2.5 kW, 0.5 m/min), joint B

The microstructure of the base metal of microalloyed, thermomechanically rolled steel S700MC is shown in Fig. 2, while the microstructures of butt joints produced by the disk laser welding are shown in Fig. 6. The microstructure of S700MC steel plate with a thickness of 5.0 mm consists mainly of fine grained ferrite with a uniform dispersion of fine carbides, Fig. 2. Additionally segregation shearing lines created as a result of the rolling process can be observed on the optical micrographs. As can be seen in Fig. 5 and 6 the microstructure of the weld metal in fusion zone (FZ), as well as the width and microstructure of heat affected zone (HAZ), were significantly dependent on the thermal conditions (heat input) of laser welding and thus subsequent cooling rates. The cooling times between 800 and 500°C were calculated for different heat inputs of autogenous disk laser welding of 5.0 mm thick butt joints of the S700MC steel in the manner described in detail in the ref 34. The results of calculations are given in the Table 5.

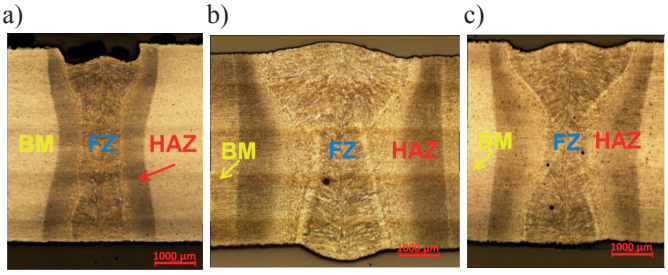

Fig. 5. Optical micrographs of the 5.0 mm thick butt joints of S700MC steel produced by autogenous laser welding (Table 4); a) joint A (3.3 kW, 1.5 m/min, heat input 132 J/mm), b) joint B (2.5 kW, 0.5 m/min, heat input 300 J/mm), c) joint C (3.3 kW, 1.0 m/min, heat input 200 J/mm)

The HAZ of joints have been recrystallized and therefore there are no segregation shearing lines, Fig. 6. The narrowest HAZ has the butt joint A welded at the lowest heat input of 132 J/mm, laser output power of 3.3 kW and welding speed 1.5 m/min, Fig. 5a and 6a. The cooling time $t_{8/5}$ calculated for the joint A is approx. 2.3 s and the width of HAZ does not exceed 0.75 mm, Fig. 6a, Table 5. The HAZ microstructure of A joint is very fine-grained with average grain size approx. 0.5 µm, so a couple of times smaller than the grain size of base metal (BM) approx. 0.8-3.5 µm, Fig. 6a. Near the fusion line coarse-grain structure can be observed but the region is very narrow with a width of one-tenth of the entire HAZ, Fig. 6b. Structure of the fine-grained region of HAZ is composed of ferrite with a uniform dispersion of fine carbides, similarly as the base metal, Fig. 2. On the other hand the structure and width of HAZ in a case of joints welded at significantly higher heat input and thus longer cooling times is different. For comparison the HAZ width of the joint C produced at heat input 198 J/mm (over twice higher that in a case of the joint A), resulted in cooling longer time $t_{8/5}$ approx. 5.2 s, is over 1.0 mm, Table 5. In this case the region of coarse-grain structure is also wider and it is approximately half the width of the entire HAZ, as can be seen in Fig. 6c. The relatively wide coarse-grain structure regions of HAZ in a case of the joint C but also joint B include polygonal ferrite grains α_{pf}, as can be seen in Fig. 6c. Close inspection of the weld metal micrographs showed clear differences in structure and grain size of the joints produced at different parameters of laser welding, thus different thermal conditions (heat input), Fig. 5 and 6. The fusion zone of the joint A produced at the lowest heat input of 132 J/mm has a columnar shape with a width approx. 1.0 mm, slightly concave face and fine-grained structure, Fig. 5a and 6b.

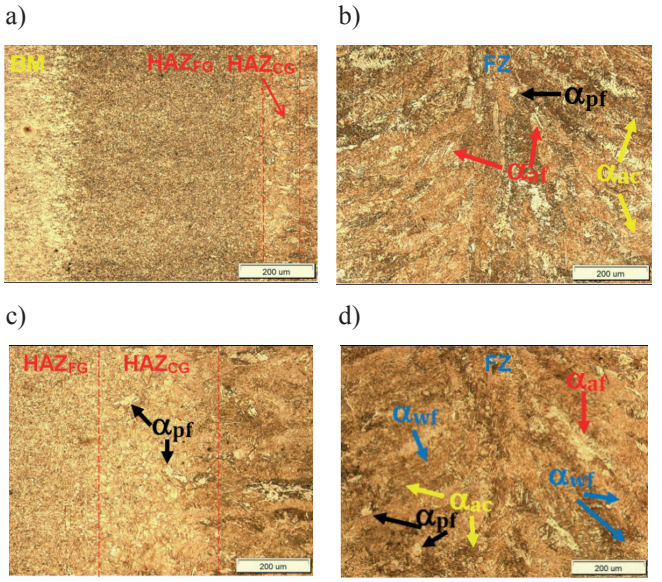

Fig. 6. Microstructure of the 5.0 mm thick butt joint of S700MC steel plate autogenously welded by the disk laser; a) HAZ of test joint A, b) FZ of test joint A, c) HAZ of test joint C, d) FZ of test joint C, HAZFG – fine-grained region of HAZ, HAZCG – coarse-grained region of HAZ, αpf – polygonal ferrite, αwf – widmanstatten ferrite, αaf – allotriomorphic ferrite, αac – acicular ferrite

TABLE 5

Values of the calculated cooling times $t_{8/5}$ during autogenous laser welding of 5.0 mm thick butt joints of S700MC steel by disk laser TruDisk 3302, Fig. 5 and 6

Test butt joint	Output laser power (W)	Welding speed (mm/min) (mm/s)	Heat input (J/mm)	HAZ width (mm)	Cooling time $t_{8/5}$ (s)
A	3300	1500 (25)	132	0.6-0.75	2.31
B	2500	500 (8.33)	300	1.5-1.75	11.94
C	3300	1000 (16.6)	198	0.87-1.15	5.20

The weld metal is free of any inclusions or porosity and consists of different types of ferrite, Fig. 5a, 6b. In this case the fraction of acicular ferrite α_{ac} is relatively high. Additionally some fraction of fine-grained allotriomorphic ferrite α_{af} (or grain boundary ferrite) and single grains of polygonal ferrite apf may be observed, Fig. 6b. On the other hand, in the case of weld metal of joint C produced at lower welding speed 1.0 m/min and heat input of 198 J/mm the acicular ferrite α_{ac} fraction is lower, Fig. 6d. Simultaneously the grains of polygonal ferrite α_{pf} are larger in size, similarly like the grains of allotriomorphic ferrite α_{af} (or grain boundary ferrite), Fig. 6d.

The microhardness distribution across the butt joints (microhardness profiles) are shown in Fig. 7. Microhardness of the base metal of 5.0 mm thick S700MC steel sheet is very

consistent in a range from 270 to about 290 HV0.2, Fig. 7. Comparison of the microhardness distribution in the HAZ and FZ of the test butt joints produced at different welding parameters indicates that the thermal conditions (heat input) of welding have a strong impact on the microhardness values measured in Vicker's scale. In a case of the joint A welded at the highest speed of 1.5 m/min and the lowest heat input of 132 J/mm the HAZ shows a tendency for increasing the microhardness, while the microhardness in the weld metal is close to the values of BM, Fig. 7a. Maximum values of microhardness approx. 350-400 HV0.2 were measured in the HAZ region adjacent to the FZ, Fig. 7a.

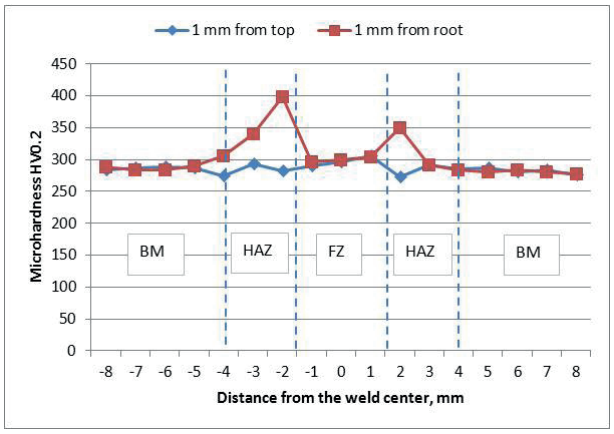

a)

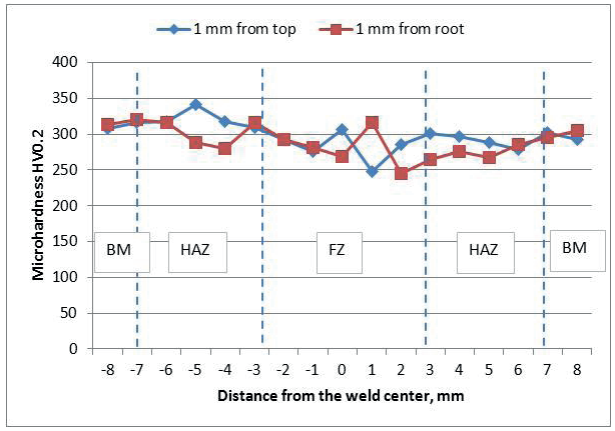

b)

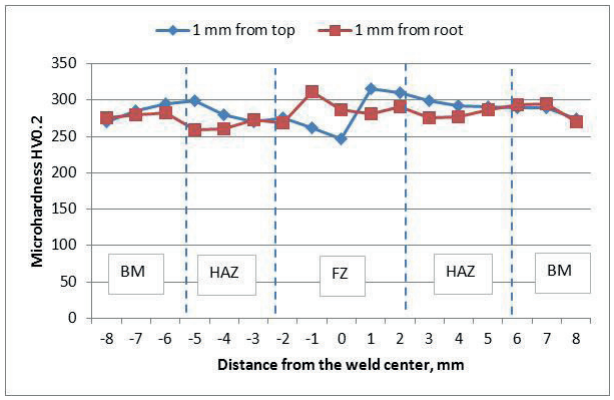

c)

Fig. 7. Microhardness distribution (profile) across the 5.0 mm thick butt joint of S700MC steel plate autogenously welded by the disk laser (Table 4); a) joint A, b) joint B, c) joint C

In contrast, the test joints welded at lower welding speed 1.0 and 0.5 m/min respectively and heat inputs 198 and 300 J/mm exhibit a slight decrease in microhardness in the FZ, Fig. 7b,c. The minimum level of microhardness measured in this case are approx. 240-250 HV0.2. Simultaneously the microhardness in HAZ does not exceed 330-340 HV0.2, Fig. 7b,c. Profile and values of the microhardness is attributed to the cooling rate and phase transformations (grain size and proportions of different types of ferrite), Fig. 6.

Two tensile samples were prepared for each of the investigated butt joints and the results are given in Table 6 and shown in Fig. 8. As can be seen, in a case of the test butt joint A welded at maximum welding speed of 1.5 m/min and thus the minimum heat input of 132 J/mm one test sample was broken in the weld metal (FZ) but the second tensile sample was broken in the base metal, Fig. 8a.

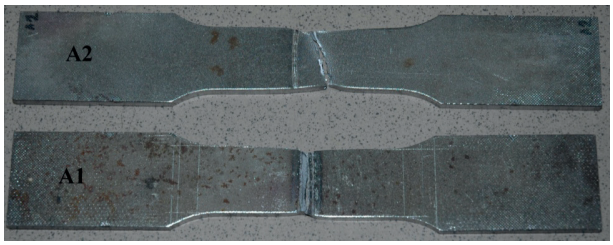

a)

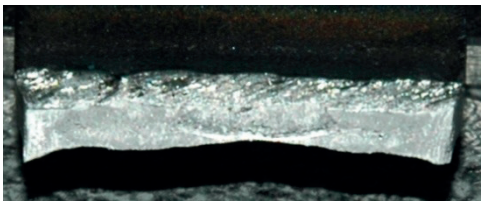

b)

Fig. 8. A view of the broken samples from the tensile tests of butt joint A welded at 3.3 kW and welding speed of 1.5 m/min (heat input of 132 J/mm, Table 6) (a) and an optical micrograph of the fracture surface (delamination can be observed) (b)

The tensile strength of these samples is above 850 MPa, Table 6. It is worth noting that the butt joint A welded at the minimum heat input showed the highest microhardness both in the FZ (weld metal) approx. 290-310 HV0.2 and in the HAZ up to 350-400 HV0.2, Fig. 6a. However, in a case of the butt joints welded at higher heat inputs all the tensile samples were broken in the FZ (weld metal), Table 6. The lowest tensile strength of 756 MPa showed the sample B2 of the joint welded at the maximum heat input of 300 J/mm, 2.5 kW and welding speed 0.5 m/min, Table 6. For comparison the tensile strength of the joint C welded at the medium heat input is just slightly lower (approx. 2.4%) than the tensile strength of the joint A. The mean tensile strength of the test joint C is approx. 836 MPa, Table 6.

TABLE 6

Results of the tensile strength test of 5.0 mm thick butt joints of S700MC steel laser welded by the disk laser, evaluated according to the PN-EN 895 standard, Fig. 8

Joint type	Sample No.	Tensile strength Rm, MPa	Place of break
A	A1	851	Weld metal
	A2	861	Base metal

B	B1	784	Weld metal
	B2	756	Weld metal
C	C1	835	Weld metal
	C2	838	Weld metal

TABLE 7
Results of the technological bend test of 5.0 mm thick butt joints of S700MC steel laser welded by the disk laser, evaluated according to the PN-EN 895 standard, Fig. 9

Joint / sample type	Test type	Bending angle, °	Remarks
A	Weld root bending	142	Longitudinal crack with a length of approx. 2.5-3 mm
	Weld face bending	151	Longitudinal crack with a length of approx. 3 mm
B	Weld root bending	55	Longitudinal fracture across the entire width
	Weld face bending	58	Longitudinal fracture across the entire width
C	Weld root bending	140	Longitudinal crack with a length of approx. 3-4 mm
	Weld face bending	145	Longitudinal crack with a length of approx. 2.5-3 mm

Fig. 9. A view of the samples after technological bend test (weld root bending) of 5.0 mm thick butt joints of S700MC steel sheets autogenous laser welded by the disk laser, evaluated according to the PN-EN 895 standard, Table 7

In general, the lower the heat input of welding, the higher the strength of the test joints in the range of welding parameters. However, it should be emphasized that the heat input, defined as the ratio of laser power and welding speed, is only an auxiliary parameter that may be applied for a comparison of welding thermal conditions only over a narrow range of laser processing parameters, as shown by previous studies discussed in the ref 34. The reason for this is the complexity of the absorption of laser radiation, heat generation and heat transfer in the region of welding, especially in a case of a keyhole welding mode. The physical processes mentioned above are influenced by many factors such as power density of the laser beam (laser radiation), temperature of the irradiated surface, time of laser beam irradiation, intensity of metal evaporation, plasma plume formation and many others [34]. It was also found that the plastically deformed metal of the tensile sample broken in the base metal, characterized by maximum tensile strength, is delaminated in the fracture zone, as shown in Fig. 8b. Delamination of the tensile sample is a result of segregation shearing lines, which can be seen in the micrographs of BM. The segregation shearing lines of BM cause anisotropy of mechanical properties and can reduce the mechanical performance of the steel plates.

TABLE 8
Results of the impact toughness test of 5.0 mm thick butt joints of S700MC steel laser welded by disk laser, evaluated according to the PN-EN 10045-1 standard, Fig. 10

Joint type/ sample No. Single value		**Absorbed impact energy, J**		**Impact toughness, J/cm²**		**Heat input of laser welding, J/mm**
		Mean value	**Single value**	**Mean value**		
A	1A	50	**49.12**	100	**98.25**	132
	2A	48.75		97.5		
	3A	48.75		97.5		
B	1B	30.5	**32.5**	61	**65**	300
	2B	32		64		
	3B	35		70		
C	1C	51.25	**54.16**	102.5	**108.25**	198
	2C	56.25		112.5		
	3C	55		110		

a) b)

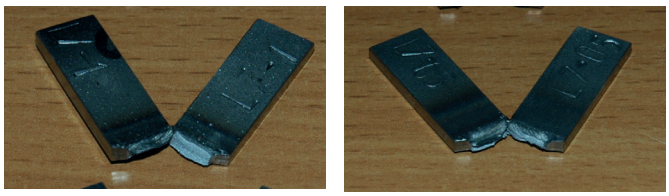

c)

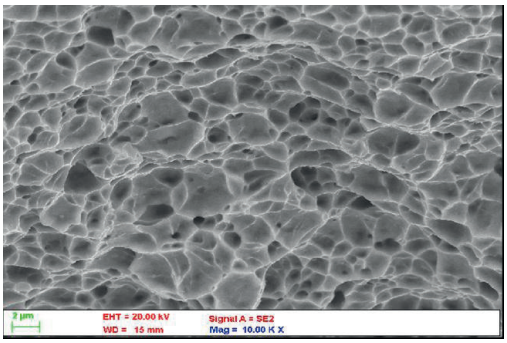

Fig. 10. A view of broken impact sample of test joint B (a) and SEM micrograph of the fracture surface of the test joint B - intercrystalline cleavage fracture (b), Table 8

Technological bend tests of the laser welded joints were performed according to the PN-EN 910:1999. Two samples were prepared for each of the examined butt joints (one for root and one for weld face bending). Samples with a width of 15.0 mm were cut in the same way as the samples for tensile tests, perpendicularly to the joint axis. Results are given in Table 7 and in Fig 9. The results of technological bend tests showed a similar trend as in the case of the tensile tests. It was found that the bending angle of test samples is related to the parameters of laser welding (heat input), Fig. 9, Table 7. The test samples of the joint B welded at maximum heat input of 300 J/mm showed the smallest bending angle approx. 55°, Fig. 9, Table 7. On the contrary, the test samples of the joint A welded at the minimum heat input showed the largest bending angle approx. 145°, Fig. 9, Table 7.

The impact toughness tests of butt joints were performed are at room temperature and the results are given in Table 8 and shown in Fig. 10. The test butt joint A welded at the lowest heat input (132 J/mm) and characterized by the highest microhardness in fusion zone and heat affected zona, as well as the highest tensile strength (851-861 MPa) and bending angle (142-151°), showed the impact toughness almost 100 J/cm^2, Table 8. The test butt joint C welded at medium heat input of laser welding (approx. 200 J/mm) showed a slightly higher impact strength at the level 108 J/cm^2, Table 8. The lowest impact toughness was reveled in a case of the test butt joint B welded at the highest heat input of 300 J/mm. In this case the impact toughness is just 65 J/cm^2, so approx. 60% of the maximum value measured for the test joint C, Table 8. A close observation of the fracture surfaces under a scanning electron microscope reveled the fracture behavior of the samples of joint B, Fig. 10c.

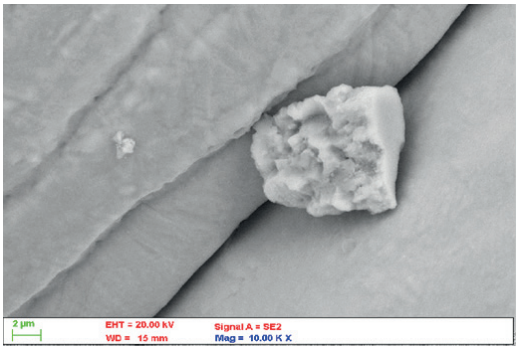

a)

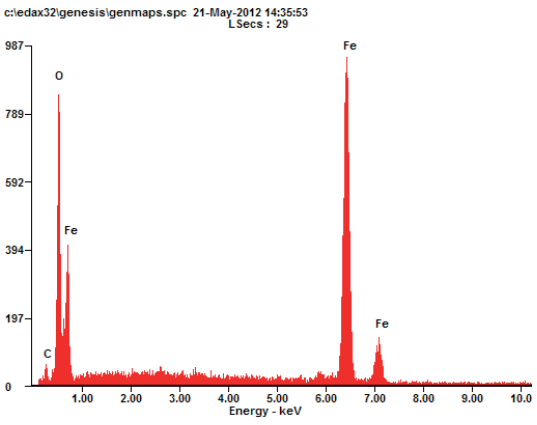

b)

Fig. 11. SEM of an inclusion on the fracture surface of broken impact sample of test joint B (a) and EDS spectra of the inclusion (b)

The fracture surface is characteristic for intercrystalline cleavage fracture of grains and subgrains boundaries. The fracture behavior of test joints is directly related to the microstructure of weld metal and heat affected zone and thus indirectly to the welding parameters, thermal conditions and heat input of laser welding. Additionally inclusions of small size were found on the fracture surfaces of the test joints, Fig. 11a. The EDS spectra of the small inclusions showed high content of oxygen in the compounds, indicating oxide nature of the inclusions, probably mainly FeO, Fig. 11b.

4. Conclusions

In this research, autogenous laser welding of butt joints of thermomechanically rolled steel S700MC was investigated. Effect of a disk laser output power and welding speed thus heat input of welding on the welding mode, fusion zone shape, microhardness profile, structure and quality of welded joints were analyzed. Mechanical performance of the butt joints was also examined. Based on the presented results of investigations the following findings can be summarized.

Autogenous laser welding of 5.0 mm thick butt joints at keyhole mode by the novel Yb:YAG disk laser provides high quality joints characterized by fine-grained structure with a large proportion of acicular ferrite, high mechanical performance.

However, ensuring high quality of welded joints requires precise selection of parameters and conditions of laser welding. Both the microstructure and mechanical performance of test joints showed a strong dependence on the welding parameters, heat input and cooling rates.

In general, the lower the heat input of Yb:YAG disk laser keyhole welding (resulted in very short cooling times $t_{8/5}$ approx. 2-5 s) the higher the mechanical performance such as tensile strength, bending angle and impact toughness.

REFERENCES

[1] A. Lisiecki, Welding of thermomechanically rolled fine-grain steel by different types of lasers, Arch. Metall. Mater. 59(4), 1625-1631 (2014). DOI: 10.2478/amm-2014-0276.

[2] A. Lisiecki, Diode laser welding of high yield steel, Proceedings of SPIE, Laser Technology 2012: Application of Lasers, 8703 (2013), DOI: 10.1117/12.2013429.

[3] K. Nishioka, K. Ichikawa, Progress in thermomechanical control of steel plates and their commercialization, Sci. Technol. Adv. Mater. 13, 023001 (2012).

[4] T. Węgrzyn, J. Piwnik, B. Łazarz, D. Hadryś, Main micro-jet cooling gases for steel welding, Arch. Metall. Mater. 58(2), 555–557 (2013).

[5] D. Janicki, Fiber laser welding of nickel based superalloy Rene 77, Proceedings of SPIE, Laser Technology 2012: Applications of Lasers, 8703 (2013) 87030Q.

[6] T. Węgrzyn, J. Mirosławski, A. Silva, D. Pinto, M. Miros, Oxide inclusions in steel welds of car body, Mat. Sci. Forum 6, 585-591 (2010).

[7] A. Kurc - Lisiecka, W. Ozgowicz, W. Ratuszek, J. Kowalska, 'Analysis of Deformation Texture in AISI 304 Steel Sheets',

Sol. St. Phenomena 203-204, 105-110 (2013).

[8] M. Bonek, The investigation of microstructures and properties of high speed steel hs6-5-2-5 after laser alloying, Arch. Metall. Mater. 59(4), 1647-1651 (2014).

[9] J. Jezierski, K. Janerka, Parameters of a Gas-Solids Jet in Pneumatic Powder Injection into Liquid Alloys with a Non-Submerged Lance, Metalurgija 54(2), 365-367 (2015).

[10] M. Bonek, L.A. Dobrzański, Characterization performance of laser melted commercial tool steels, Mat. Sci. Forum 654-656, 1848-1851 (2010).

[11] W. Sitek, L.A. Dobrzański, Comparison of hardenability calculation methods of the heat-treatable constructional steels, J. Mat. Proc. Tech. 64(1-3), 117-126 (1995).

[12] T. Węgrzyn, J. Piwnik, D. Hadryś. Oxygen in steel WMD after welding with micro-jet cooling, Arch. Metall. Mater. 58(4), 1067–1070 (2013).

[13] B. Oleksiak, G. Siwiec, A. Blacha-Grzechnik, J. Wieczorek, The obtained of concentrates containing precious metals for pyrometallurgical processing, Metalurgija 53(4), 605-608 (2014).

[14] J. Górka, Analysis of simulated welding thermal cycles S700MC using a thermal imaging camera, Adv. Mat. Res. ISI Proceedings 837, 375-380 (2014).

[15] G. Golański, A. Zieliński, J. Słania, J. Jasak, Mechanical Properties of VM12 steel after 30 000hrs of ageing at 600°C temperature, Arch. Metall. Mater. 59(4), 1357-1360 (2014).

[16] G. Golański, P. Gawień, J. Słania, Examination of Coil Pipe Butt Joint Made of 7CrMoVTib10 - 10(T24) Steel After Service, Arch. Metall. Mater. 57(2), 1067–1070 (2012).

[17] B. Oleksiak, J. Labaj, J. Wieczorek, A. Blacha – Grzechnik, R. Burdzik, Surface tension of cu-bi alloys and wettability in a liquid alloy - refractory material - gaseous phase system, Arch. Metall. Mater. 59(1), 281-285 (2014).

[18] T. Węgrzyn, J. Piwnik, Low alloy steel welding with micro-jet cooling, Arch. Metall. Mater. 57(2), 539–543 (2012).

[19] J. Ni, Z. Li, J. Huang, Y. Wu, Strengthening behavior analysis of weld metal of laser hybrid welding for microalloyed steel, Materials and Design 31, 4876–4880 (2010).

[20] B. Oleksiak, M. Koziol, J. Wieczorek, M. Krupa, P. Folęga, Strength of briquettes made of cu concentrate and carbon-bearing materials, Metalurgija 54(1), 95-97 (2015).

[21] M. Gao, X. Zeng, Q. Hu, J. Yan, Laser-TIG hybrid welding of ultra-fine grained steel, J. Mat. Proc. Tech. 209, 785-791 (2009).

[22] G. Golański, J. Jasak, J. Słania, Microstructure, properties and welding of T24 steel - critical review, Kovove Materialy 52, 99-106 (2014).

[23] R. Burdzik, Ł. Konieczny, Research on structure, propagation and exposure to general vibration in passenger car for different damping parameters, J. of Vibroengineering 15(4), 1680-1688 (2013).

[24] W. Tarasiuk, B. Szczucka–Lasota, J. Piwnik, W. Majewski, Tribological Properties of Super Field Weld with Micro-Jet Process, Adv. Mat. Res. 1036, 452-457 (2014).

[25] D. Janicki, Disk laser welding of armor steel, Arch. Metall. Mater. 59(4), 1641-1646 (2014).

[26] R. Burdzik, Ł. Konieczny, T. Figlus, Activities of Transport Telematics, Book Series: Communications in Computer and Information Science 395, 418-425 (2013).

[27] R. Burdzik, Research on the influence of engine rotational speed to the vibration penetration into the driver via feet - multidimensional analysis, J. of Vibroengineering 15(4), 2114-2123 (2013).

[28] R.S. Sharma, P. Molian, Weldability of advanced high strength steels using an Yb:YAG disk laser, J. Mat. Proc. Tech. 211, 1888-1897 (2011).

[29] R. Burdzik, Z. Stanik, J. Warczek, Method of assessing the impact of material properties on the propagation of vibrations excited with a single force impulse, Arch. Metall. Mater. 57(2), 409–416 (2012).

[30] J. Bodzenta, A. Kaźmierczak, T. Kruczek, Analysis of thermograms based on FFT algorithm, Journal de Physique IV 129, 201-206 (2005).

[31] A. Grajcar, M. Różański, S. Stano, A. Kowalski, B. Grzegor czyk: 'Effect of Heat Input on Microstructure and Hardness Distribution of Laser Welded Si-Al TRIP-Type Steel' Adv. in Mat. Sci. and Eng. 2014 (2014),

[32] M. Musztyfaga, L.A. Dobrzański, S. Rusz, M. Staszuk, Application examples for the different measurement modes of electrical properties of the solar cells, Arch. Metall. Mater. 59, (1) 247-252 (2014).

[33] A. Grabowski, M. Nowak, J. Śleziona, Optical and conductive properties of AlSialloy/SiCp composites: application in modeling CO_2 laser processing of composites, Optics and Lasers in Engineering 43, 233–246 (2005).

[34] A. Lisiecki, Effect of heat input during disk laser bead-on-plate welding of thermomechanically rolled steel on penetration characteristics and porosity formation in the weld metal, Arch. Metall. Mater. (in press).

Received: 20 October 2014.